

TURBO-CODES AND HIGH SPECTRAL EFFICIENCY MODULATION

Stéphane Le Goff, Alain Glavieux and Claude Berrou

Stéphane Le Goff and Claude Berrou, Integrated Circuits for Telecommunications Laboratory

Alain Glavieux, Digital Communication Laboratory

TELECOM BRETAGNE, FRANCE TELECOM UNIVERSITY

BP 832 - 29285 BREST, FRANCE

ABSTRACT This paper presents a new coding scheme based on the association of a turbo-code [1] with a bandwidth-efficient modulation. It is shown that the new coding scheme provides a substantial coding gain both on Gaussian channels and Rayleigh channels. On a Gaussian channel, it outperforms 64-state trellis-coded modulation (TCM) by 2.5 dB at the bit error rate (BER) of 10^{-6} . On a Rayleigh fading channel, it outperforms 64-state TCM optimized for that environment.

1 - INTRODUCTION

Turbo-codes, newly introduced by Berrou *et al* [1], are binary error-correcting codes built from the parallel concatenation of two recursive systematic convolutional codes and using a feedback decoder. Simulations over a Gaussian channel, using binary modulations (2-PSK or 4-PSK), have shown that turbo-codes possess an error-correcting capability unmatched at the present time.

In order to improve the transmission spectral efficiency, it is interesting to combine turbo-codes with a bandwidth-efficient modulation. In this paper, we investigate in particular combining a turbo-code of rate R with QAM constellations, over Gaussian and Rayleigh channels. This approach can be considered as an alternative to the conventional Trellis Coded Modulation (TCM). It is generally simpler to implement and moreover results in better performance than TCM, on both Gaussian and Rayleigh channels.

2 - TURBO-CODES PRINCIPLE

Turbo-codes result from concatenation of two recursive systematic convolutional (RSC) codes. In Fig. 1, an example of a rate $R = 1/3$ standard turbo-encoder is shown. Two RSC elementary encoders C_1 and C_2 , with the same constraint length $K = 5$ and the same polynomial generators (23, 35) are used. Both elementary encoder C_1 and C_2 receive the same information string $\{d_k\}$ but arranged in a different sequence due to the presence of an interleaver I_1 and a delay line L_1 . Given an input bit d_k , the encoder outputs at time k are equal to d_k itself since encoding is systematic, and the outputs c_k^1 and c_k^2 of the elementary encoders C_1 and C_2 .

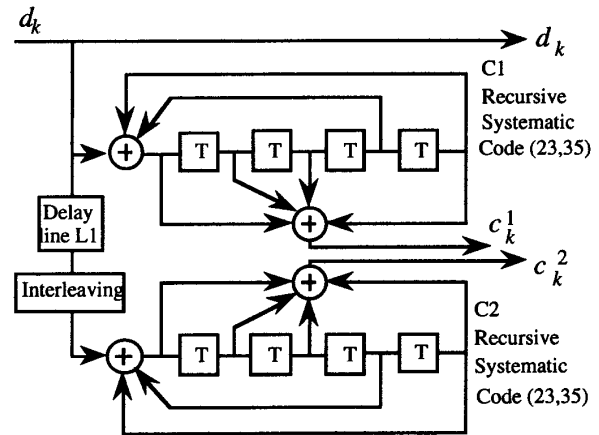


Figure 1 Rate $R=1/3$ standard turbo-encoder

The turbo-decoder is made up of P pipelined identical modules as depicted in Fig. 2 and thus the turbo decoder structure is modular [1]. The p th module input at time k is made up of demodulator outputs $(X_k)_{p-1}$ and $(Y_k)_{p-1}$ through a delay line and of extrinsic information $(Z_k)_{p-1}$ provided by the $(p-1)$ th module. Extrinsic information $(Z_k)_{p-1}$ is new information concerning bit d_k but affected by a noise weakly correlated with the noise that perturbs the observations $(X_k)_{p-1}$ and $(Y_k)_{p-1}$. Therefore extrinsic information and observations provided by the demodulator can be used jointly by the $(p-1)$ th module for carrying out a new decoding of bit d_k . The extrinsic information acts as a diversity effect and can therefore improve the decoder performance. Each module consists of two elementary decoders (DEC₁ and DEC₂) in a serial concatenation scheme. Both elementary decoders provide a soft decision and use a low complexity soft output Viterbi algorithm [2].

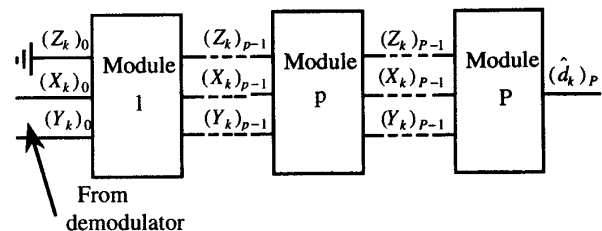


Figure 2 Turbo-decoder with P pipelined identical modules

3 - ASSOCIATION OF A TURBO-CODE WITH A MULTILEVEL MODULATION

We now consider the association of M -state QAM or PSK ($M = 2^m$) modulation and rate $R = (m - \tilde{m}) / m$ encoder built from a standard turbo-encoder by using puncturing technique as depicted in Fig. 3.

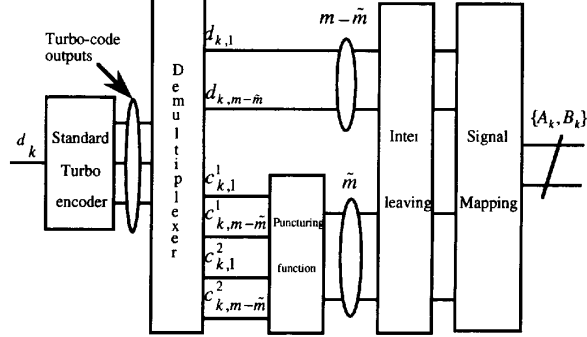


Figure 3 Association of a turbo-code with a multilevel modulation

The puncturing function is inserted at the standard turbo-encoder output and thus it is possible to obtain a large code family, with various rates R . In order to obtain symbols affected with uncorrelated noises at the turbo-decoder input, an interleaver I_2 has to be inserted between the puncturing function and the modulator. With this approach, the transmission spectral efficiency η is equal to :

$$\eta = R \log_2 M \quad (1)$$

Each point of the QAM (or PSK) constellation is represented by a couple of real-valued symbols $\{A_k, B_k\}$ at time k coded by a set $\{u_{k,i}\}$, $i = 1 \dots m$ of m bits according to a Gray code. The redundant bits provided by the punctured turbo-encoder are associated to the highest protected bit $u_{k,i}$.

For example, for a 16-QAM constellation with Gray coding depicted on Fig. 4, and for a rate $R=3/4$ turbo-encoder, parameters m and \tilde{m} are respectively equal to 4 and 1.

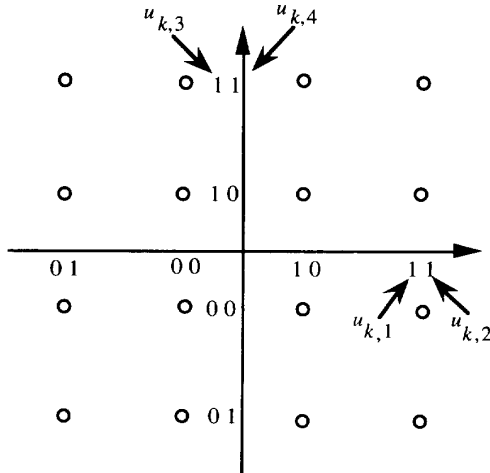


Figure 4 16-QAM constellation with GRAY coding

According to notations of Fig. 3, we have $u_{k,i} = d_{k,i}$; $i = 2, 3, 4$; $u_{k,1} = c_{k,1}^1$ and then $u_{k+1,1} = d_{k+1,1}$; $i=2,3,4$ $u_{k+1,1} = c_{k+1,1}^2$ and so on.

4 - RECEIVER AND TURBO-DECODER STRUCTURE

Consider a coherent receiver, the in-phase and quadrature demodulator outputs X_k and Y_k are equal to :

$$X_k = \alpha_k A_k + I_k \quad (2)$$

$$Y_k = \alpha_k B_k + Q_k$$

where α_k is a Rayleigh random variable for a Rayleigh channel and a constant equal to 1 for a Gaussian channel, and I_k, Q_k are two uncorrelated gaussian noises, with zero mean, variance σ_N^2 and independent of variable α_k .

We assume that a pragmatic approach [3] is taken, so that the input turbo-decoder is made up of soft decisions associated to each turbo-encoder output bit. From observation of $\{X_k, Y_k\}$, the Logarithm of Likelihood Ratio (LLR) associated with each bit $u_{k,i}$, $i = 1 \dots m$ can be determined and used as a relevant soft decision by the turbo-decoder as depicted in Fig. 5.

$$\Lambda(u_{k,i}) = K \log \frac{P_r\{u_{k,i} = 1 / X_k, Y_k\}}{P_r\{u_{k,i} = 0 / X_k, Y_k\}}, \quad i = 1 \dots m \quad (3)$$

where K is a constant.

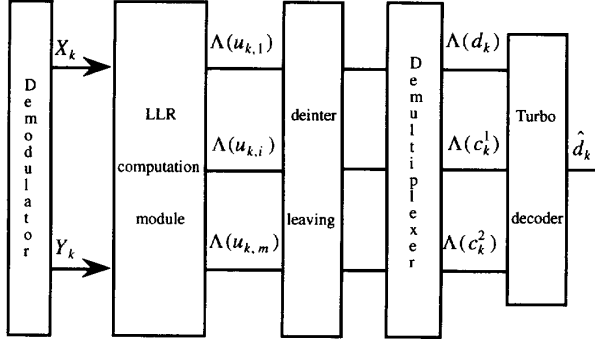


Figure 5 Pragmatic decoder structure

Unfortunately, the computation of m quantities $\Lambda(u_{k,i})$ leads to relatively complicated expressions which depend on signal-to-noise ratio (SNR) and channel characteristics (Gaussian or Rayleigh channel). Nevertheless it is possible to approximate these expressions by simpler relations. For example consider the case of square M -QAM constellations with $M = 2^m$ and $m = 2p$.

4 - 1 Gaussian channel

By taking into account the fact that the observation $\{X_k, Y_k\}$ is affected by two independent gaussian noises with identical variance σ_N^2 , and using Bayes' rule, the LLR $\Lambda(u_{k,i})$ associated to bit $u_{k,i}$, $i = 1 \dots p$ depends only on observation X_k .

$$\Lambda(u_{k,i}) = K \log \frac{\sum_{i=1}^{2^{p-1}} \exp \left\{ -\frac{1}{2\sigma_N^2} (X_k - a_{1,i})^2 \right\}}{\sum_{i=1}^{2^{p-1}} \exp \left\{ -\frac{1}{2\sigma_N^2} (X_k - a_{0,i})^2 \right\}}, \quad i = 1 \dots p \quad (4)$$

where $a_{1,i}$ and $a_{0,i}$ respectively represent the realization of symbols A_k conditionally on $u_{k,i} = 1$ and $u_{k,i} = 0$. In the same way, the LLR associated to bit $u_{k,i+p}$, $i = 1 \dots p$ depends only on observation Y_k and has the same expression as $\Lambda(u_{k,i})$ but with Y_k substituted for X_k , and $b_{1,i}$ and $b_{0,i}$ for $a_{1,i}$ and $a_{0,i}$ respectively.

A good approximation of the LLR $\Lambda(u_{k,i})$ for $K = \sigma_N^2 / 2$ can be achieved using the following expressions :

$$\begin{aligned} \Lambda(u_{k,1}) &= |X_k| - 2^{p-1} \\ \Lambda(u_{k,i}) &= |\Lambda(u_{k,i-1})| - 2^{p-i}, \quad i = 2 \dots (p-1) \\ \Lambda(u_{k,p}) &= X_k \end{aligned} \quad (5-a)$$

and :

$$\begin{aligned} \Lambda(u_{k,1+p}) &= |Y_k| - 2^{p-1} \\ \Lambda(u_{k,i+p}) &= |\Lambda(u_{k,i-1+p})| - 2^{p-i}, \quad i = 2 \dots (p-1) \\ \Lambda(u_{k,2p}) &= Y_k \end{aligned} \quad (5-b)$$

In Fig 6, the LLR $\Lambda(u_{k,i})$ associated to bit $u_{k,i}$, $i = 1, 2$ is plotted for a 16-QAM constellation and for a $E_b / N_0 = 4$ dB, where E_b is the energy received per information bit and N_0 the one-sided noise power spectral density.

$$\frac{E_b}{N_0} = \frac{(M-1)}{3 \log_2 M} \frac{1}{\sigma_N^2} \quad (6)$$

Fig. 6 shows that relations (5-a, 5-b) appear to be good approximations to the LLR even for rather low SNR values.

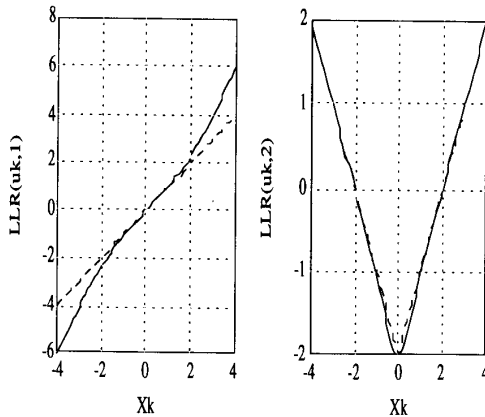


Figure 6 Logarithm of the Likelihood ratio corresponding to bit $u_{k,i}$, $i=1,2$ for a 16-QAM modulation at $E_b/N_0=4$ dB (Full line LLR from relation 4; dashed line LLR from relations 5-a, 5-b)

Unfortunately, with the pragmatic approach, the LLRs $\Lambda(u_{k,i})$ associated to bits $u_{k,i}$, $i = 1 \dots p$ (respectively bits $u_{k,i+p}$, $i = 1 \dots p$) are affected by correlated noises, which

accounts for the interleaver inserted after the puncturing function (Fig.3). Moreover, in the general case, for a given couple (A_k, B_k) , the $\Lambda(u_{k,i})$ variables are not gaussian except for $i = p$ and $i = 2p$ and thus the soft-output Viterbi algorithm used in each elementary decoder DEC₁ and DEC₂ is no longer optimal. Nevertheless for large SNR values, the $\Lambda(u_{k,i})$ variables are close to gaussian variables with the same variance, and therefore the turbo-decoder performance is still quite attractive with the pragmatic approach.

4 -2 Rayleigh channel

We assume a memoryless Rayleigh fading channel whose α_k is known by the receiver. Under this assumption, relations (2) can be normalized by α_k . That is :

$$\begin{aligned} x_k &= A_k + i_k \\ y_k &= B_k + q_k \end{aligned} \quad (7)$$

where :

$$x_k = \frac{X_k}{\alpha_k}, \quad y_k = \frac{Y_k}{\alpha_k} \quad \text{and} \quad i_k = \frac{I_k}{\alpha_k}, \quad q_k = \frac{Q_k}{\alpha_k} \quad (8)$$

Relations (7) are similar to those obtained over a Gaussian channel, but i_k and q_k are now nonstationary noises whose variance depends on time k through variable α_k .

$$E_{\alpha_k} \{ (i_k)^2 \} = \frac{\sigma_N^2}{\alpha_k^2}, \quad E_{\alpha_k} \{ (q_k)^2 \} = \frac{\sigma_N^2}{\alpha_k^2} \quad (9)$$

If we use relations (5-a) and (5-b) to determine simpler expressions for the LLR, we have now to take into account the variance of noises i_k and q_k for the metric computation $M_{k,i}^j$ in the low complexity soft-output Viterbi algorithm.

$$M_{k,i}^j = j \Lambda(u_{k,i}) \frac{\alpha_k^2}{\sigma_N^2} \quad j = -1, 1; \quad i = 1 \dots p \quad (10)$$

With the pragmatic approach, the turbo-decoder structure is optimized for binary transmission (2-PSK or QPSK) over a Gaussian channel. Thus the metrics used in the turbo-decoder are independent of the noise variance and are equal to :

$$M_{k,i}^j = j \Lambda(u_{k,i}) \quad j = -1, 1 \quad (11)$$

By using the following notations :

$$\begin{aligned} \tilde{\Lambda}(u_{k,i}) &= \alpha_k^2 \Lambda(u_{k,i}) \quad i = 1 \dots p \\ \tilde{\Lambda}(u_{k,i+p}) &= \alpha_k^2 \Lambda(u_{k,i+p}) \quad i = 1 \dots p \end{aligned} \quad (12)$$

the metric (10) can be evaluated from relation (11) by substituting $\tilde{\Lambda}(\cdot)$ for $\Lambda(\cdot)$. Thus the turbo decoder optimized for a Gaussian channel, is also optimal for a Rayleigh channel if $\tilde{\Lambda}(u_{k,i})$ is used as the LLR expression.

5 - RESULTS

A rate $R=1/3$ standard turbo-encoder, made up of two elementary encoders with the same constraint length $K=5$ and the same polynomial generators (23,35) is considered in the following simulations. For different spectral efficiencies obtained by puncturing redundant bits at the standard turbo-encoder output, we have computed the Bit Error Rate (BER) using the Monte Carlo method as a function of E_b / N_0 . In order to compare the performance of this new coded scheme

with conventional TCM, we have also plotted the BER of the 64-state TCM and of the equivalent uncoded modulation (providing the same spectral efficiency).

5 - 1 Gaussian channel

The nonuniform interleaver I_1 is composed of a (64x64) matrix whereas the uniform interleaver I_2 uses a smaller matrix, with p rows and a number of columns equal to several times the encoder constraint length K . Turbo decoding is performed in 3 iterations and the BER curves, for a spectral efficiency of 2, 3, 4 bit/s/Hz, are plotted in Figs. 7 to 9.

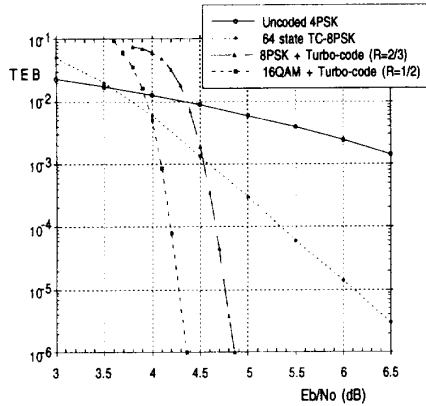


Figure 7 BER of a rate $R=1/2$ turbo-code associated with a 16-QAM versus E_b/N_0 over a Gaussian channel (2bit/s/Hz spectral efficiency)

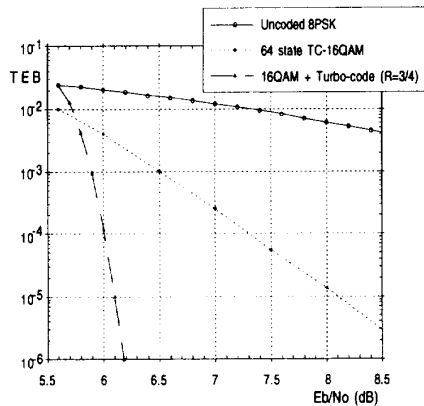


Figure 8 BER of a rate $R=3/4$ turbo-code associated with a 16-QAM versus E_b/N_0 over a Gaussian channel (3bit/s/Hz spectral efficiency)

We can notice that for both spectral efficiencies considered and for a BER less than 10^{-3} , the turbo code performance is always better than the 64-state TCM. The main results obtained, in terms of coding gain (expressed in dB) are indicated in the table I. Thus, for a 3bit/s/Hz spectral efficiency and a 16-QAM constellation, the turbo code gives a

coding gain equal to 2.5 dB compared to a 64-state TC 8-PSK at a BER equal to 10^{-6} .

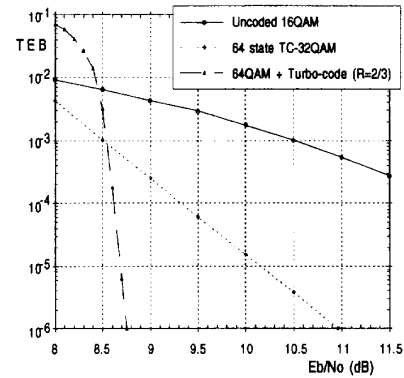


Figure 9 BER of a rate $R=2/3$ turbo-code associated with a 64-QAM versus E_b/N_0 over a Gaussian channel (4bit/s/Hz spectral efficiency)

For higher spectral efficiencies (>3 bit/s/Hz) the coding gain is weaker, but we can see that the BER slope is still larger with a turbo-code than with 64-state TCM.

We have also evaluated the performance of a rate $R=2/3$ turbo-code associated with a 8-PSK (2 bit/s/Hz spectral efficiency). The coding gain is smaller than with the rate $R=1/2$ turbo-code associated with 16-QAM. However the turbo-code solution always gives a better performance than the conventional 64-state TC 8-PSK.

Finally, we have checked the usefulness of interleaver I_2 over a gaussian channel. Indeed without the interleaver I_2 , the $\Lambda(u_{k,i})$ at the DEC1 input are just correlated over p values and thanks to interleaver I_1 , the samples at the DEC2 input are almost uncorrelated. Therefore, it is possible to drop the interleaver I_2 over a gaussian channel.

Turbo code rate	1/2	2/3	3/4	2/3
Modulation	16-QAM	8-PSK	16-QAM	64-QAM
Spectral efficiency	2	2	3	4
Coding gain at 10^{-6} over uncoded modulation	6.0 dB	5.5 dB	7.8 dB	5.8 dB
Coding gain at 10^{-6} over 64 state TCM	2.4 dB	1.9 dB	2.6 dB	2.2 dB

Table I Coding gain at a BER equal to 10^{-6} for a turbo-code over a Gaussian channel

5 - 2 Rayleigh channel

The curves of BER for a spectral efficiency equal to 2, 3 and 4 bit/s/Hz, are plotted in Figs. 10 to 12 as a function of \bar{E}_b/N_0 where :

$$\bar{E}_b = 2\sigma^2 E_b \quad \text{with} \quad E\{\alpha_k^2\} = 2\sigma^2 = 1 \quad (13)$$

We have also plotted in Fig. 11 the BER of a 64-state TC 16-QAM [4], and respectively in Figs. 10 and 12 the BER of a trellis-coded 4-ASK and 8-ASK multilevel modulation with 64 states [5].

The turbo decoding is performed in 4 iterations and the uniform interleaver I_2 is now made up with a matrix having $2p$ rows (the same number of columns as for the Gaussian channel) in order to obtain uncorrelated Rayleigh variables α_k at the decoder DEC1 input. We can see that over a Rayleigh channel, the interleaver I_2 is necessary to achieve the best performance.

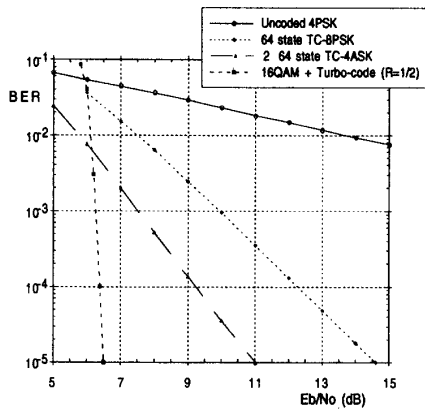


Figure 10 BER of a rate $R=1/2$ turbo-code associated with a 16-QAM versus E_b/N_0 over a Rayleigh channel (2bit/s/Hz spectral efficiency)

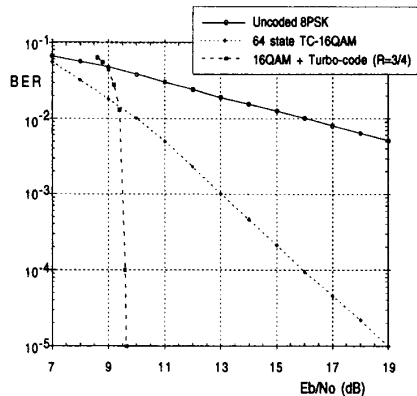


Figure 11 BER of a rate $R=3/4$ turbo-code associated with a 16-QAM versus E_b/N_0 over a Rayleigh channel (3bit/s/Hz spectral efficiency)

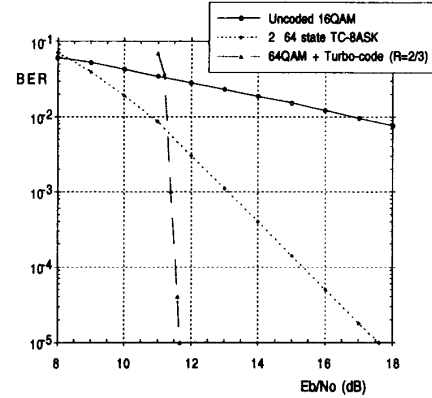


Figure 12 BER of a rate $R=2/3$ turbo-code associated with a 64-QAM versus E_b/N_0 over a Rayleigh channel (4bit/s/Hz spectral efficiency)

In all considered cases, the turbo-codes provide a better performance than the 64-state TCM, when the BER is less than 10^{-3} . For example for a spectral efficiency of 3 bit/s/Hz, the coding gain compared to 64-state TCM (codes of DU and VUCETI [4]) is equal to 9.5 dB!

6 - CONCLUSIONS

In this paper we have presented a new coding scheme using the association of a turbo-code with a quadrature amplitude modulation. For both Gaussian and Rayleigh channels, the performance of this new error correcting scheme is always better than the 64-state TCM, at BER values less than 10^{-3} . The high performance of this new error correcting scheme is essentially due to the good distance properties of the turbo-code which are obtained using a nonuniform interleaver I_1 . Moreover, with a pragmatic approach, the turbo-decoder structure depends neither on the M parameter nor on channel type, and therefore, a single VLSI decoder can be suitable for both spectral efficiencies. Finally a turbo-code associated to M -QAM also makes high speed links possible since a turbo-decoder with 16-state trellis, is much simpler to implement than a 64 state TCM.

REFERENCES

- [1] C. Berrou, A. Glavieux and P. Thitimajshima, "Near Shannon limit error-correcting coding and decoding : Turbo-codes", *ICC'93, Conf. Rec. pp.1064-1070, Geneva, May 1993*.
- [2] C. Berrou, P. Adde, E. Angui and S. Faudeil, "A low complexity soft-output Viterbi decoder architecture", *ICC'93 Conf. Rec., pp.737-740, Geneva, May 1993*.
- [3] A.J. Viterbi, E. Zehavi, R. Padovani and J.K. Wolf, "A pragmatic approach to trellis-coded modulation", *IEEE Commun. Mag., Vol. 27, N°7, pp. 11-19, July 1989*.
- [4] J. Du and B. Vucetic "New 16-QAM trellis codes for fading channels", *Electronics letters, Vol 26, N°16, pp. 1267-1269, August 1990*.
- [5] J.F. H  lard, "Modulations cod  es en treillis associ  es    un multiplex de porteuses orthogonales en pr  sence de canaux affect  s de trajets multiples", Th  se de doctorat de l'Universit   de Rennes I, N   d'ordre : 776, pp. 5-12, Mai 1992.